2023 EAGE ANNUAL
84TH CONFERENCE & EXHIBITION
VIENNA | AUSTRIA

Wave-equation deconvolution for angle-dependent reflectivity and internal multiple prediction

G. Poole[1], J. Tickle[1]

[1] CGG

Summary

Short period multiple prediction for land data is challenging due to poor imaging of the shallow multiple generators as well little information about the down-going reflection at the weathering layer. Based on multiple imaging of the shallow section, surface-related wave-equation deconvolution has been used in recent years to improve multiple prediction in such areas. We improve the accuracy of wave-equation deconvolution to include an angle dependency of the multiple generator reflectivity. In addition, we modify the approach to handle internal multiple predictions where the lower-generator is provided by surface-related wave-equation deconvolution, and the upper-reflectivity is derived through least-squares inversion. The combined benefit of these two approaches is demonstrated on a land dataset from south Oman.

Wave-equation deconvolution for angle-dependent reflectivity and internal multiple prediction

Introduction

Most free-surface multiple prediction approaches assume that the multiple generators have been adequately recorded as primaries (for example Berkhout and Verschuur, 1997 or Pica et al., 2005). These methods also assume that the upper-reflecting surface may be approximated by a horizontal perfectly reflecting water-air boundary. In the marine context, such assumptions are generally met for long-period multiple generators. In shallow water settings, primaries are generally not sufficiently well recorded at small enough reflection angles to use for multiple prediction, and model-based (Wang et al., 2011 or Wiggins, 1988) or deconvolution (Biersteker, 2001 or Poole, 2019) approaches are typically adopted. In land settings, short period multiple prediction is further complicated by the weathering layer as well as more limitation on the availability of shallow primary recordings at small reflection angles. Li et al. (2021) presented an application of surface-related wave-equation deconvolution (Poole, 2019) in a land setting. The approach derived a shallow reflectivity responsible for multiple prediction, which combined the multiple generators along with weathering layer effects.

In this paper, we extend the surface-related wave-equation deconvolution methodology to include angle-dependent reflectivity. In addition, we formulate wave-equation deconvolution for the prediction of short-period internal multiples, generated in the shallow section.

Method

Following the notation of Poole et al. (2022), wave-equation multiple modelling may be described by the following three steps, also refer to Equation 1:

Step 1) Forward propagate each frequency, f, in the input data to every location (coordinates x, y, z) in the subsurface, populating D_{Φ}.
Step 2) Multiply forward propagated data by the reflectivity image, r, to produce a reflecting wavefield.
Step 3) Forward propagate reflecting wavefield back to the surface using propagation operator, Φ.

The result is reverse Fourier transformed from the frequency domain, *f*, to the time domain, *t*, using operator F^{-1}, resulting in a multiple model in the space-time domain, m_{surf}.

$$m_{surf}(t,x,y) = F^{-1}\Phi(f,x,y,z)D_{\Phi}(f,x,y,z)r(x,y,z) \quad (1)$$

As given by Equation 2, wave-equation deconvolution derives the optimal reflectivity image to minimize the misfit, ε, with the recorded data, d.

$$\varepsilon(r) = [d(t,x,y) - F^{-1}\Phi(f,x,y,z)D_{\Phi}(f,x,y,z)r(x,y,z)]^2 \quad (2)$$

The wave-equation deconvolution (WEDecon) approach involves reflectivity inversion based on Equation 2, followed by multiple modelling based on Equation 1, followed by subtraction.

Angle dependent reflectivity

A single-valued reflectivity limits the multiple prediction to the same reflection amplitude at all reflection angles. In addition, inaccuracies in the shallow velocity model may blur the reflectivity and reduce the multiple prediction accuracy. One way to overcome this limitation involves redefining Equation 2 to simultaneously derive near, mid, and far angle reflectivities (r_n, r_m, and r_f respectively) as shown in Equation 3. In this formulation, multiple models from each reflectivity are combined using space-time mute operators for each angle range (M_n, M_m, and M_f). The angle ranges for each operator may be, for example, 0-12°, 12-24°, and 24-36°.

$$\varepsilon(r_n, r_m, r_f) = \left[d - [M_n \quad M_m \quad M_f] F^{-1}\Phi \begin{bmatrix} D_{\Phi} & 0 & 0 \\ 0 & D_{\Phi} & 0 \\ 0 & 0 & D_{\Phi} \end{bmatrix} \begin{bmatrix} r_n \\ r_m \\ r_f \end{bmatrix} \right]^2 \quad (3)$$

An alternative and more pragmatic formulation, which solves for each angle range separately, is given by Equations 4, 5, and 6. In this case, the muting operators act as sparseness weights, such that the least squares solution for each reflectivity is only determined by the input data within each angle range (d_n,

d_m, and d_f). After deriving each reflectivity, the approach continues by predicting three multiple models which are finally combined and adaptively subtracted from the input data.

$$\varepsilon(r_n) = [d_n - M_n F^{-1} \Phi D_\Phi r_n]^2 \quad (4)$$
$$\varepsilon(r_m) = [d_m - M_m F^{-1} \Phi D_\Phi r_m]^2 \quad (5)$$
$$\varepsilon(r_f) = \left[d_f - M_f F^{-1} \Phi D_\Phi r_f\right]^2 \quad (6)$$

Internal multiples

As well as surface-related multiples, many datasets are contaminated by internal multiples, which contain their down-going reflection within the subsurface. Pica and Delmas (2008) defined a wave-equation internal multiple modelling approach using upper and lower primary images. The approach is illustrated in Figure 1 and involves the following steps.

Step b) Backwards propagate recorded data into upper reflectivity (shown in blue).
Step c) Reflect downwards from upper reflectivity.
Step d) Forward propagate downwards reflecting wavefield into lower reflectivity (shown in green).
Step e) Reflect forwards propagated wavefield upwards in lower reflectivity.
Step f) Forwards propagate upwards reflecting wavefield to the receivers.

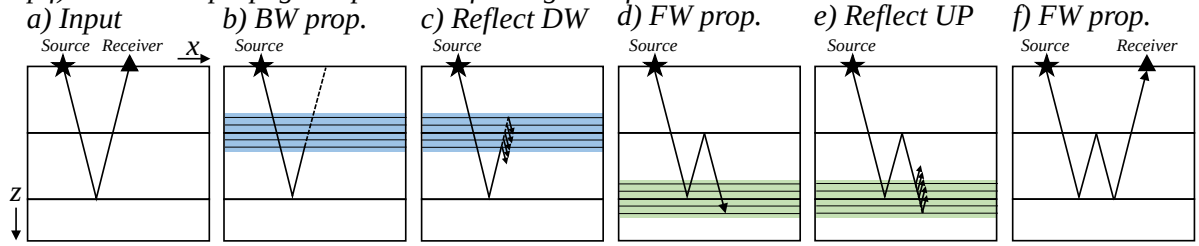

Figure 1 *Illustration of wave-equation multiple modelling based on Pica and Delmas (2008).*

Seismic data may not be available at small enough reflection angles for imaging the upper and lower reflectivities. We propose to use reflectivity from standard surface-related WEDecon (Poole, 2019) for the lower reflectivity and to derive the upper reflectivity using the internal WEDecon approach given below. The lower reflectivity may be used directly or interpreted, for example, using horizon tracking. Given in Equation 7, the internal WEDecon approach derives upper reflectivity, r_u, based on backwards propagated input data, $D_{-\Phi}$, and the lower reflectivity, R_l, from surface-related WEDecon.

$$\varepsilon(r_u) = [d(t,x,y) - F^{-1}\Phi(f,x,y,z)R_l(x,y,z)\Phi(f,x,y,z)D_{-\Phi}(f,x,y,z)r_u(x,y,z)]^2 \quad (7)$$

Once the upper reflectivity has been derived using least-squares inversion, we may model internal multiples, m_{inter}, using Equation 8. The internal multiples may then be subtracted from the input data.

$$m_{inter}(t,x,y) = F^{-1}\Phi(f,x,y,z)R_l(x,y,z)\Phi(f,x,y,z)D_{-\Phi}(f,x,y,z)r_u(x,y,z) \quad (8)$$

Data example

The data example comes from a land dataset acquired in south Oman with a 25 m × 50 m shot carpet recorded by geophones with 25 m × 200 m sampling. Figure 2a shows a raw migration of the input data which is seen to be heavily contaminated by short period multiples throughout. The auto-correlation QC highlights the level of reverberating energy present in this data. Figure 2b shows results after surface consistent deconvolution (Garceran and Le Meur, 2012) using a 28 ms gap in the shallow section and a 48 ms gap in the deeper section. Surface-consistent deconvolution has attenuated some of the lower frequency multiples, but high multiple levels are still present in the data, particularly at the higher frequencies. The auto-correlation QC shows the partial attenuation of lower frequency multiples. Figure 2c shows the data after standard surface-related WEDecon where a significant reduction in the level of residual multiples can be appreciated, see the black arrows, particularly visible on the auto-correlation.

For comparison, angle-dependent surface-related WEDecon was applied to the input data. Figure 3 compares reflectivity images from standard and angle-dependent surface-related WEDecon. Key events can be observed on all reflectivities, sometimes changing slightly in amplitude or timing, as highlighted by the arrows. In general, the near offsets exhibit stronger focussing, indicating a higher level of reverberating energy in the near offset data.

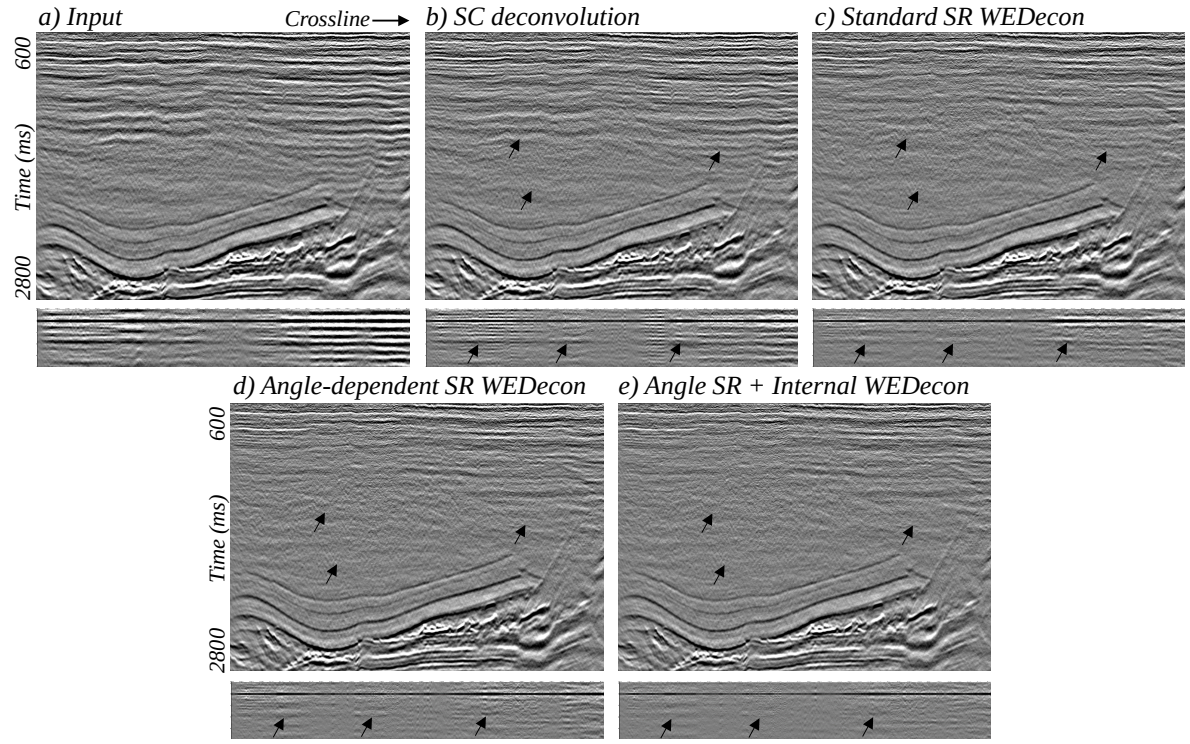

Figure 2 *Raw migration QC for: a) Input, b) Surface-consistent deconvolution, c) Standard surface-related WEDecon, d) Angle-dependent surface-related WEDecon, and e) Angle-dependent surface-related WEDecon followed by internal WEDecon. Trace-by-trace normalised auto-correlation QCs with lag –100 to +400 ms are given below each result.*

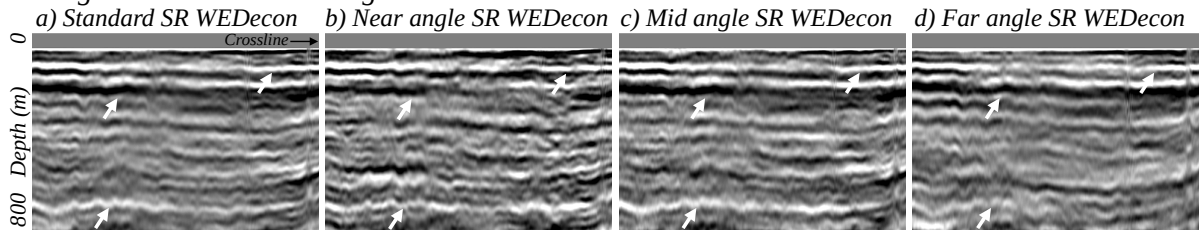

Figure 3 *Surface-related WEDecon reflectivity images for: a) Standard WEDecon (0-36°), b) Near angle WEDecon (0-12°), c) Mid angle WEDecon (12-24°), and d) Far angle WEDecon (24-36°).*

Multiple modelling was performed for the three reflectivity images and combined using the respective angle mutes. Shown in Figure 2d, the resulting multiple model was adaptively subtracted from the input. Comparing standard WEDecon (Figure 2c) with the angle-dependent WEDecon (Figure 2d), we can observe a further reduction in the level of residual multiples, as highlighted by the black arrows.

Following angle-dependent WEDecon, the data was input to internal WEDecon. In this case, a potential upper generator (*H1*) and two potential lower generators (*H2* and *H3*) were identified from the surface-related WEDecon image (Figure 4a). The lower generators were interpreted as horizons to remove the potential effect of the weathering layer from the surface-related WEDecon image. The upper reflectivity was then derived using Equation 7 based on internal multiples between *H1-H2* (Figure 4b) and *H1-H3* (Figure 4c). The upper reflectivities given in Figures 4b and 4c show a nice similarity, adding confidence to the result. Internal multiples were modelled based on Equation 8 and mildly adaptively subtracted from the data after surface-related angle dependent WEDecon (Figure 2e). The result shows an incremental reduction in multiple content compared to Figure 2d, highlighted by the black arrows.

Although the multiple content was significantly reduced through cascaded application of the proposed techniques, a significant level of multiple remained in the dataset. For this reason, post-migration targeted multiple attenuation followed by signal enhancement (Retailleau et al., 2014) was applied. Figure 5 compares post-migration processing results with no pre-migration demultiple, after standard surface-related WEDecon, and after the proposed flow. As highlighted by the arrows, we observe an incremental improvement in the level of residual multiple with the proposed flow.

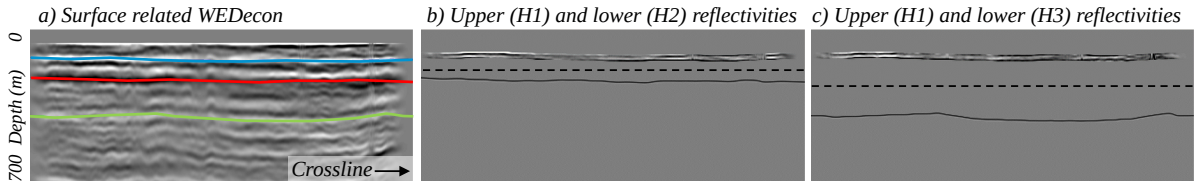

Figure 4 *WEDecon reflectivities for: a) Surface-related WEDecon; horizons H1, H2 and H3 shown in blue, red, and green respectively, b) H1 reflectivity for internal multiples H1→H2 (H2 shown below dashed line), and c) H1 reflectivity for internal multiples H1→H3 (H3 shown below dashed line).*

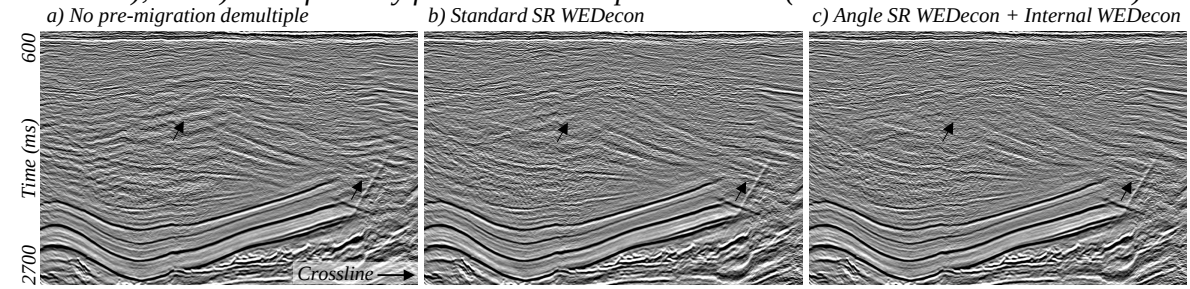

Figure 5 *Final imaging results for: a) No pre-migration demultiple, b) Standard surface-related WEDecon, and c) Angle-dependent surface-related WEDecon followed by internal WEDecon.*

Conclusions

We have introduced inversion-driven wave-equation demultiple approaches with angle-dependent reflectivity and internal multiple prediction. The approaches were applied to a land dataset from south Oman, providing a reduction in multiple content compared to traditional methods. After post-processing the results were appreciable, but more marginal. This is still a challenging area for future focus.

Acknowledgements

The data is from Petroleum Development Oman. We thank Petroleum Development Oman, the Oman Ministry of Energy and Minerals and CGG for permission to publish this paper. Thanks to Brandon Li for help producing the real data examples.

References

Berkhout, A. J. and Verschuur, D. J. [1997] Estimation of multiple scattering by iterative inversion, Part I: theoretical consideration. *Geophysics*, **62**(5), 1586-1595.

Biersteker, J. [2001] MAGIC: Shell's surface multiple attenuation technique. *71st SEG Annual International Meeting*, Expanded Abstracts, 1301-1304.

Garceran, K. and Le Meur, D. [2012] Simultaneous Joint Inversion for Surface Consistent Amplitude and Deconvolution. *74th EAGE Conference and Exhibition*, Extended Abstracts, C015.

Li., B., Miorali, M., Mills, K. and Poole, G. [2021] 3D surface related multiple attenuation for land data using least-squares multiple imaging. *PESGB PETEX Conference*, Extended Abstracts.

Pica, A., Poulain, G., David, B., Magesan, M., Baldock, S., Weisser, T., Hugonnet, P. and Herrmann, P. [2005] 3D surface-related multiple modeling, principles and results. *75th SEG Annual International Meeting*, Expanded Abstracts, 2080-2083.

Pica, A. and Delmas, L. [2008] Wave equation based internal multiple modeling in 3D. *78th SEG Annual International Meeting*, Expanded Abstracts, 2476-2480.

Poole, G. [2019] Shallow water surface related multiple attenuation using multi-sailline 3D deconvolution imaging. *81st EAGE Conference and Exhibition*, Extended Abstracts, Tu R1 5.

Poole, G., Farshad, M., Jin, Z. and Li, B. [2022] Wave-equation deconvolution: A short-period demultiple tool for streamer, OBN and land environments. *First Break*, **22**, 59-64.

Retailleau, M., Shorter, J., Farran, H., Hugonnet., P., Wa Hong, T., Benjamin, N, and Pica, A. [2014] Two strategies for attenuating internal multiples in land data. *International Petroleum Technology Conference*, IPTC 17451.

Wang, P., Jin, H., Xu, S. and Zhang, Y. [2011] Model-based water-layer demultiple. *81st SEG Annual International Meeting*, Expanded Abstracts, 3551-3555.

Wiggins, W. [1988] Attenuation of complex water-bottom multiples by wave-equation-based prediction and subtraction. *Geophysics*, **53**, 1527-1539.